J. Phys. Chem. A **2004,** *108,* 2555−2558

Isomer Stability of N_{24}, N_{30}, and N_{36} Cages: Cylindrical versus Spherical Structure

Douglas L. Strout*

Department of Physical Sciences, Alabama State University, Montgomery, Alabama 36101

Received: December 16, 2003

Nitrogen molecules have been extensively studied for their potential as high energy density materials (HEDM). One of the major issues in the study of N_x all-nitrogen molecules is the determination of stable structures. In this study, various cage isomers of N_{24}, N_{30}, and N_{36} are examined for the purposes of determining relative thermodynamic stability. Trends in thermodynamic stability make possible the identification of structural features that lead to stable molecules. All of the molecules in this study have three-coordinate nitrogen with all N−N single bonds. Thermodynamic stability is determined by theoretical calculations employing Hartree−Fock theory (HF), density functional theory (B3LYP), and Moller−Plesset perturbation theory (up to MP4). The correlation-consistent basis sets of Dunning are employed. The major result of this study is the identification of cylinder-shaped molecules that are substantially more stable than more spherically shaped isomers.

Introduction

Nitrogen molecules have been the subjects of many recent studies because of their potential as high energy density materials (HEDM). An all-nitrogen molecule N_x can undergo the reaction $N_x \rightarrow (x/2)N_2$, a reaction that can be exothermic by 50 kcal/mol or more per nitrogen atom.[1,2] To be a practical energy source, however, a molecule N_x would have to resist dissociation well enough to be a stable fuel. Theoretical studies[3−7] have shown that numerous N_x molecules are not sufficiently stable to be practical HEDM, including cyclic and acyclic isomers with eight to twelve atoms. Cage isomers of N_8 and N_{12} have also been shown[7−10] by theoretical calculations to be unstable. Experimental progress in the synthesis of nitrogen molecules has been very encouraging, with the N_5^+ and N_5^- ions having been recently produced[11,12] in the laboratory. Those experimental successes have sparked theoretical studies[13,14] on other potential all-nitrogen molecules, and future developments in experiment and theory will further broaden the horizons of all-nitrogen research.

The stability properties of N_x molecules have also been extensively studied in a computational survey[15] of various structural forms with up to 20 atoms. Cyclic, acyclic, and cage isomers have been examined to determine the bonding properties and energetics over a wide range of molecules. A more recent computational study[16] of cage isomers of N_{12} examined the specific structural features that lead to the most stable molecules among the three-coordinate nitrogen cages. Those results showed that molecules with the most pentagons in the nitrogen network tend to be the most stable, with a secondary stabilizing effect due to triangles in the cage structure.

In the current study, cage isomers of N_{24}, N_{30}, and N_{36} are examined by theoretical calculations to determine their relative thermodynamic stability. Such cages have only N−N single bonds between three-coordinate nitrogen atoms, and the surface of each cage consists of a network of polygons. For the purpose of this study, the polygons shall be limited to triangles, squares, pentagons, and hexagons. For each molecule, n_3, n_4, n_5, and n_6 shall represent the number of three-, four-, five-, and six-sided polygons, respectively, in that molecule. Within that framework, the polygons in each N_x molecule are subject to the following mathematical bounds:

$$3n_3 + 2n_4 + n_5 = 12 \text{ (Euler's Theorem)} \qquad (1)$$

$$n_3 + n_4 + n_5 + n_6 = (x/2) + 2 \qquad (14 \text{ for } N_{24}, 17 \text{ for } N_{30}, 20 \text{ for } N_{36}) \quad (2)$$

The relationships between stability and the various types of polygons will indicate which structural features tend to stabilize an all-nitrogen cage.

Computational Details

Geometries are optimized using Hartree−Fock (HF) theory, the B3LYP density functional method,[17,18] and second-order Moller−Plesset perturbation theory[19] (MP2). (Several geometry optimizations failed for B3LYP and MP2, which have a bond-lengthening effect relative to HF theory, and this lengthening of bonds can lead to dissociative geometry optimizations.) Single energy points are calculated with fourth-order Moller−Plesset perturbation theory[19] (MP4(SDQ)). The basis sets[20] are the correlation-consistent sets (CC−PVDZ and CC−PVTZ) of Dunning. Calculations in this study are performed with the Gaussian 98 and Gaussian 03 quantum chemistry software packages.[21,22]

Results and Discussion

Six N_{24} cages are under consideration in this study. Each cage shall be labeled by its $n_3n_4n_5n_6$ polygon specifications. Figure 1 shows an isomer with the specifications 00(12)2 (that is, twelve pentagons and two hexagons). The molecule has D_{6d} point group symmetry and is analogous to a previously studied C_{24} molecule.[23] Figure 2 shows an octahedral (O_h point group) cage with 0608 specifications. This molecule also has an analogue in a previous C_{24} study.[23] Figures 3 and 4 show two different cages with 2066 specifications and D_{3d} point group symmetry. The molecule in Figure 3 shall be denoted 2066P because the two triangles are each surrounded by pentagons,

---

* E-mail: dstrout@asunet.alasu.edu.

10.1021/jp0378889 CCC: $27.50

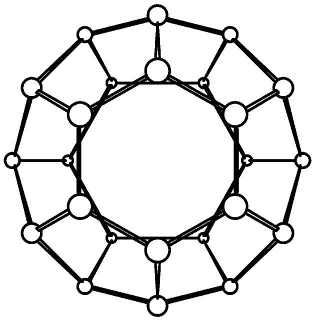

Figure 1. N$_{24}$ 00(12)2 fullerene isomer (D_{6d} symmetry).

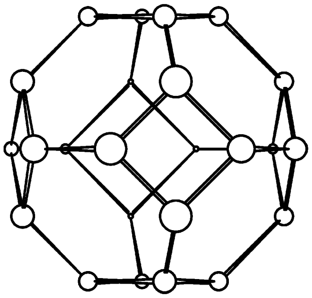

Figure 2. N$_{24}$ 0608 isomer (O_h symmetry).

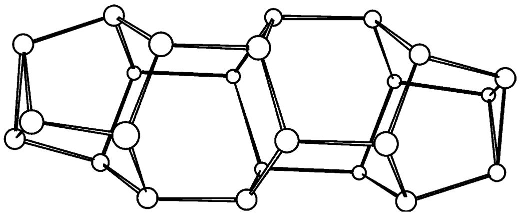

Figure 3. N$_{24}$ 2066P isomer (D_{3d} symmetry).

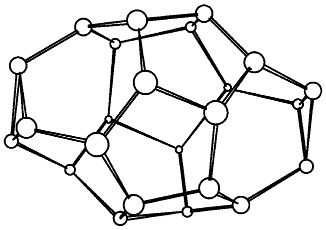

Figure 4. N$_{24}$ 2066H isomer (D_{3d} symmetry).

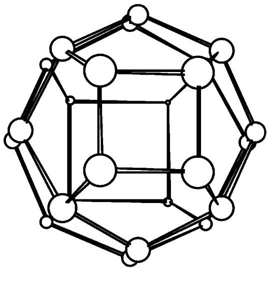

Figure 5. N$_{24}$ 0284 isomer (D_{4h} symmetry).

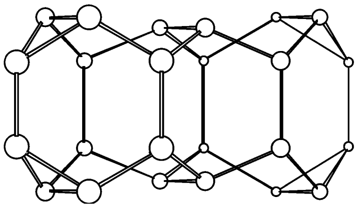

Figure 6. N$_{24}$ 400(10) isomer (D_{2h} symmetry).

TABLE 1: Relative Energies of N$_{24}$ Cages, Calculated with CC−PVDZ Basis Set (energies in kcal/mol)

	isomer specifications					
method	00(12)2	2066P	2066H	0608	0284	400(10)
HF	0.0	−104.1	+31.4	+205.6	−30.4	+20.6
B3LYP	0.0	−81.4	*a*	*a*	−23.6	+11.0
MP2	0.0	−111.7	*a*	*a*	*a*	*a*
MP4//HF	0.0	−109.8	+22.2	+203.7	−32.0	+6.7
MP4//B3LYP	0.0	−107.3	*a*	*a*	−30.3	+8.2
MP4//MP2	0.0	−102.9	*a*	*a*	*a*	*a*

[a] Result unavailable due to failed geometry optimization.

TABLE 2: Relative Energies of N$_{24}$ Cages, Calculated with CC−PVTZ Basis Set (energies in kcal/mol)

	isomer specifications					
method	00(12)2	2066P	2066H	0608	0284	400(10)
HF	0.0	−97.1	+33.4	+205.1	−28.3	+28.3
B3LYP	0.0	−77.7	*a*	*a*	−22.4	+13.2
MP2	0.0	−112.5	*a*	*a*	*a*	*a*
MP4//HF	0.0	−105.3	+23.5	+202.1	−32.0	+12.2
MP4//B3LYP	0.0	−104.8	*a*	*a*	−30.8	+12.3
MP4//MP2	0.0	−100.1	*a*	*a*	*a*	*a*

[a] Result unavailable due to failed geometry optimization.

and the molecule in Figure 4 shall be called 2066H because the triangles are surrounded by hexagons. Figure 5 shows a molecule with D_{4h} symmetry and 0284 specifications, and Figure 6 depicts an isomer with 400(10) specifications (four triangles, 10 hexagons) and D_{2h} symmetry. All six molecules have been confirmed as minima at the HF/CC−PVDZ level of theory.

The energy results from calculations with the CC−PVDZ basis set are shown in Table 1. The results indicate that the most stable isomer, by far, is the 2066P isomer. The least stable isomer is 0608, more than 300 kcal/mol above 2066P (in fact, 0608 is more than 200 kcal/mol above 00(12)2, compared with less than 30 kcal/mol for the carbon analogues[23]). The HF, B3LYP, and MP2 methods disagree with each other by 20−30 kcal/mol, but MP4 energies show that 2066P is more stable than 00(12)2 by 100−110 kcal, regardless of the choice of optimized geometry. Therefore, the isomer with the most pentagons is NOT the most stable at this molecule size. The 2066P, with two triangles and six pentagons, is the most stable, but the 2066H, which also has two triangles and six pentagons, is not nearly as stable as 2066P. So it is not simply the presence of triangles or the presence of pentagons that leads to stability, but rather the structural group consisting of triangles surrounded by pentagons. That structural arrangement of triangles and pentagons forms a “cap” on either end of the 2066P. Between those “caps” is a tube of hexagonal nitrogen.

Table 2 shows results from calculations with the CC−PVTZ basis set. The additional basis functions have only a moderate effect, with basis set effects being less than 10 kcal/mol across the board. Further basis set increases are unlikely to produce significant changes in relative isomer energies. Even with the larger basis sets, the elongated, cylindrical 2066P is much more stable than more spherical isomers such as 00(12)2. Cylindrical structure tends to concentrate cage strain (as in the triangular caps of 2066P) rather than distribute it evenly, so the stability of 2066P indicates that an even distribution of cage strain is not a significant contributor to the stability of N$_{24}$ cages.

Four N$_{30}$ cages and three N$_{36}$ cages are examined in this study. The four N$_{30}$ cages include a cylindrical structure with polygon specifications 2069 and three fullerene-like isomers with specifications 00(12)5. Figure 7 shows the 2069 cylinder (D_{3h} symmetry), Figure 8 depicts a 00(12)5 fullerene with D_{5h}

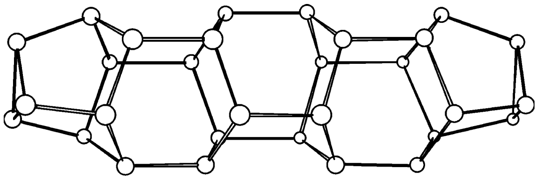

Figure 7. N_{30} 2069 isomer (D_{3h} symmetry).

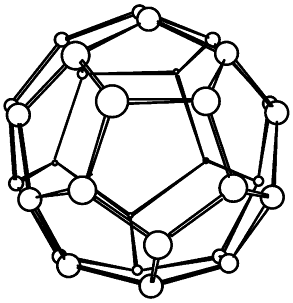

Figure 8. N_{30} 00(12)5 fullerene isomer (D_{5h} symmetry).

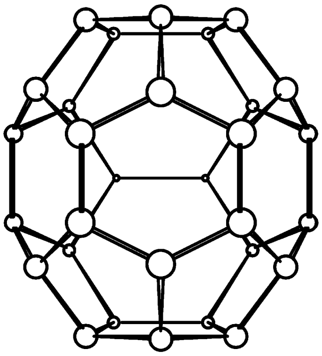

Figure 9. N_{30} 00(12)5 fullerene isomer (C_{2v} symmetry #1).

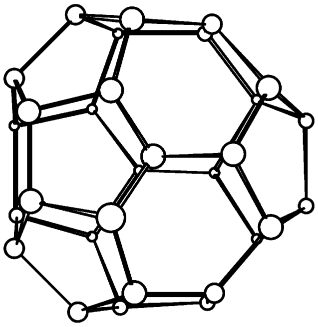

Figure 10. N_{30} 00(12)5 fullerene isomer (C_{2v} symmetry #2).

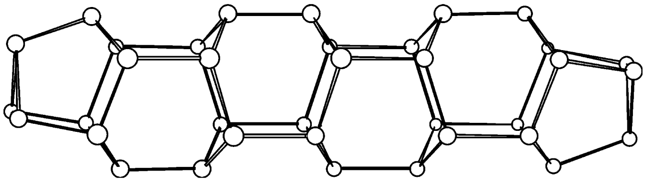

Figure 11. N_{36} 206(12) isomer (D_{3d} symmetry).

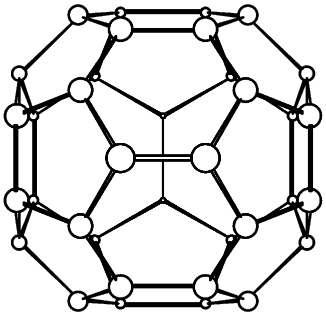

Figure 12. N_{36} 00(12)8 fullerene isomer (D_{2d} symmetry).

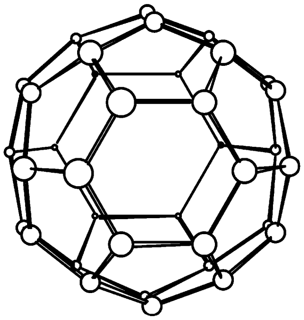

Figure 13. N_{36} 00(12)8 fullerene isomer (D_{6h} symmetry).

TABLE 3: Relative Energies of N_{30} Cages, Calculated with CC−PVDZ Basis Set (energies in kcal/mol)

	cylindrical	fullerene-like isomers		
method	2069	D_{5h}	C_{2v} #1 (Figure 9)	C_{2v} #2 (Figure 10)
HF	0.0	+186.0	+220.3	+102.4
B3LYP	0.0	+137.7	*a*	*a*
B3LYP//HF	0.0	+149.9	+179.5	+80.5
MP4//HF	0.0	+185.7	+219.5	+91.8
MP4//B3LYP	0.0	+178.8	*a*	*a*

[a] Result unavailable due to failed geometry optimization.

TABLE 4: Relative Energies of N_{36} Cages, Calculated with CC−PVDZ Basis Set (energies in kcal/mol)

	cylindrical	fullerene-like isomers	
method	206(12)	D_{2d}	D_{6h}
HF	0.0	+395.7	+389.2
B3LYP//HF	0.0	+324.4	+317.0
MP4//HF	0.0	+387.7	+379.7

symmetry, and Figures 9 and 10 show two different fullerene-like structures with C_{2v} symmetry. The three N_{36} cages include cylindrical isomers with 206(12) specifications (Figure 11), a 00(12)8 fullerene-like isomer with D_{2d} symmetry (Figure 12), and another fullerene-like isomer with D_{6h} symmetry (Figure 13).

Tables 3 and 4 show the computational results for N_{30} and N_{36}, respectively, with the CC−PVDZ basis set, and the results follow the corresponding results for N_{24}. At each molecule size, the cylindrical isomer is by far the most stable compared with the more spherical isomers, and in fact, the stability advantage for the cylinder increases with increasing molecule size. The results for N_{24} and N_{30} are comparable, with the cylindrical structures 2066P and 2069 having a stability advantage of about 100 kcal/mol with HF and MP4 and 80 kcal/mol with B3LYP, relative to their respective fullerene counterparts. The 206(12) cylindrical N_{36}, on the other hand, has more than a 300 kcal/mol advantage over the representative fullerene-like molecules at that size. It is likely that further increases in molecule size will result in even greater energetic advantage for the cylindrical molecules. (Basis set effects were not calculated for N_{30} and N_{36} since the N_{24} results show that larger basis sets do not significantly alter the outcome of the calculations.)

These results are very sensible in light of the geometric properties of spheroidal molecules. As molecule size increases, the curvature of the “sphere” decreases and the bonding environment of each three-coordinate atom approaches (in the infinite limit) a flat, trigonal planar arrangement. For a carbon fullerene, this is ideal because the natural state of three-coordinate carbon is graphite, which is planar. As a result, the stability of spheroidal carbon fullerenes of increasing size approaches the stability of graphite. However, three-coordinate nitrogen favors a pyramidal, ammonia-like environment, which will not occur for a sufficiently large spheroid. Large nitrogen cages N_x favor a more cylindrical structure, which allows for a higher degree of pyramidalization of the individual nitrogen atoms. The result is a large stability advantage for the 2066 N_{24}, 2069 N_{30}, and 206(12) N_{36} cylinders over their spheroidal counterparts.

Conclusion

Clearly, the number of pentagons is not the primary factor determining the stability of N_{24}, N_{30}, and N_{36} cage molecules. At smaller molecule sizes, such as N_{12}, the pentagons are the dominant stabilizing features. For larger molecules, a more complex picture emerges, with triangles playing at least as important a role as the pentagons. Furthermore, the specific arrangement of pentagons relative to triangles plays a central role, leading to cylindrical structures in which nitrogen atoms keep their preferred pyramidal environments. It is probable that this cylindrical, hexagonal form of nitrogen (with triangle-pentagon "caps") is thermodynamically preferred among all large N_x molecules with all single bonds. The highly symmetric cylindrical structures of the type shown in this study exist only when x is a multiple of six, but similar cylindrical forms may exist at other sizes as well and have a similar stability advantage.

Acknowledgment. The Alabama Supercomputer Authority is gratefully acknowledged for a grant of computer time on the Cray SV1 in Huntsville, AL. This work was partially supported by the National Computational Science Alliance under Grant CHE030332N and utilized the IBM p690 cluster in Champaign, IL. This work was also supported by the National Institutes of Health (NIH/NCMHHD Grant 1P20MD000547-01). The taxpayers of the state of Alabama in particular and the United States in general are also gratefully acknowledged.

References and Notes

(1) Fau, S.; Bartlett, R. J. *J. Phys. Chem. A* **2001**, *105*, 4096.

(2) Tian, A.; Ding, F.; Zhang, L.; Xie, Y.; Schaefer, H. F., III. *J. Phys. Chem. A* **1997**, *101*, 1946.

(3) Chung, G.; Schmidt, M. W.; Gordon, M. S. *J. Phys. Chem. A* **2000**, *104*, 5647.

(4) Strout, D. L. *J. Phys. Chem. A* **2002**, *106*, 816.

(5) Thompson, M. D.; Bledson, T. M.; Strout, D. L. *J. Phys. Chem. A* **2002**, *106*, 6880.

(6) Li, Q. S.; Liu, Y. D. *Chem. Phys. Lett.* **2002**, *353*, 204.

(7) Li, Q. S.; Zhao, J. F. *J. Chem. Phys. A* **2002**, *106*, 5367.

(8) Gagliardi, L.; Evangelisti, S.; Widmark, P. O.; Roos, B. O. *Theor. Chem. Acc.* **1997**, *97*, 136.

(9) Gagliardi, L.; Evangelisti, S.; Bernhardsson, A.; Lindh, R.; Roos, B. O. *Int. J. Quantum Chem.* **2000**, *77*, 311.

(10) Schmidt, M. W.; Gordon, M. S.; Boatz, J. A. *Int. J. Quantum Chem.* **2000**, *76*, 434.

(11) Christe, K. O.; Wilson, W. W.; Sheehy, J. A.; Boatz, J. A. *Angew. Chem., Int. Ed.* **1999**, *38*, 2004.

(12) Vij, A.; Pavlovich, J. G.; Wilson, W. W.; Vij, V.; Christe, K. O. *Angew. Chem., Int. Ed.* **2002**, *41*, 3051; Butler, R. N.; Stephens, J. C.; Burke, L. A. *Chem. Commun.* **2003**, *8*, 1016.

(13) Fau, S.; Bartlett, R. J. *J. Phys. Chem. A* **2001**, *105*, 4096.

(14) Fau, S.; Wilson, K. J.; Bartlett, R. J. *J. Phys. Chem. A* **2002**, *106*, 4639.

(15) Glukhovtsev, M. N.; Jiao, H.; Schleyer, P. v. R. *Inorg. Chem.* **1996**, *35*, 7124.

(16) Bruney, L. Y.; Bledson, T. M.; Strout, D. L. *Inorg. Chem.* **2003**, *42*, 8117.

(17) Becke, A. D. *J. Chem. Phys.* **1993**, *98*, 5648.

(18) Lee, C.; Yang, W.; Parr, R. G. *Phys. Rev. B* **1988**, *37*, 785.

(19) Moller, C.; Plesset, M. S. *Phys. Rev.* **1934**, *46*, 618.

(20) Dunning, T. H. Jr. *J. Chem. Phys.* **1989**, *90*, 1007.

(21) Frisch, M. J.; Trucks, G. W.; Schlegel, H. B.; Scuseria, G. E.; Robb, M. A.; Cheeseman, J. R.; Zakrzewski, V. G.; Montgomery, J. A., Jr.; Stratmann, R. E.; Burant, J. C.; Dapprich, S.; Millam, J. M.; Daniels, A. D.; Kudin, K. N.; Strain, M. C.; Farkas, O.; Tomasi, J.; Barone, V.; Cossi, M.; Cammi, R.; Mennucci, B.; Pomelli, C.; Adamo, C.; Clifford, S.; Ochterski, J.; Petersson, G. A.; Ayala, P. Y.; Cui, Q.; Morokuma, K.; Malick, D. K.; Rabuck, A. D.; Raghavachari, K.; Foresman, J. B.; Cioslowski, J.; Ortiz, J. V.; Stefanov, B. B.; Liu, G.; Liashenko, A.; Piskorz, P.; Komaromi, I.; Gomperts, R.; Martin, R. L.; Fox, D. J.; Keith, T.; Al-Laham, M. A.; Peng, C. Y.; Nanayakkara, A.; Gonzalez, C.; Challacombe, M.; Gill, P. M. W.; Johnson, B. G.; Chen, W.; Wong, M. W.; Andres, J. L.; Head-Gordon, M.; Replogle, E. S.; Pople, J. A. *Gaussian 98*, revision A.7; Gaussian, Inc.: Pittsburgh, PA, 1998.

(22) Frisch, M. J.; Trucks, G. W.; Schlegel, H. B.; Scuseria, G. E.; Robb, M. A.; Cheeseman, J. R.; Montgomery, J. A., Jr.; Vreven, T.; Kudin, K. N.; Burant, J. C.; Millam, J. M.; Iyengar, S. S.; Tomasi, J.; Barone, V.; Mennucci, B.; Cossi, M.; Scalmani, G.; Rega, N.; Petersson, G. A.; Nakatsuji, H.; Hada, M.; Ehara, M.; Toyota, K.; Fukuda, R.; Hasegawa, J.; Ishida, M.; Nakajima, T.; Honda, Y.; Kitao, O.; Nakai, H.; Klene, M.; Li, X.; Knox, J. E.; Hratchian, H. P.; Cross, J. B.; Adamo, C.; Jaramillo, J.; Gomperts, R.; Stratmann, R. E.; Yazyev, O.; Austin, A. J.; Cammi, R.; Pomelli, C.; Ochterski, J. W.; Ayala, P. Y.; Morokuma, K.; Voth, G. A.; Salvador, P.; Dannenberg, J. J.; Zakrzewski, V. G.; Dapprich, S.; Daniels, A. D.; Strain, M. C.; Farkas, O.; Malick, D. K.; Rabuck, A. D.; Raghavachari, K.; Foresman, J. B.; Ortiz, J. V.; Cui, Q.; Baboul, A. G.; Clifford, S.; Cioslowski, J.; Stefanov, B. B.; Liu, G.; Liashenko, A.; Piskorz, P.; Komaromi, I.; Martin, R. L.; Fox, D. J.; Keith, T.; Al-Laham, M. A.; Peng, C. Y.; Nanayakkara, A.; Challacombe, M.; Gill, P. M. W.; Johnson, B.; Chen, W.; Wong, M. W.; Gonzalez, C.; Pople, J. A. *Gaussian 03, Revision B.01*; Gaussian, Inc.: Pittsburgh, PA, 2003.

(23) Raghavachari, K.; Zhang, B.; Pople, J. A.; Johnson, B. G.; Gill, P. M. W. *Chem. Phys. Lett.* **1994**, *220*, 385.